water

MDPI

Article

Inundation Analysis of the Oda River Basin in Japan during the Flood Event of 6–7 July 2018 Utilizing Local and Global Hydrographic Data

Shakti P. C. *, Hideyuki Kamimera and Ryohei Misumi

National Research Institute for Earth Science and Disaster Resilience (NIED), Tsukuba 305-0006, Japan; kamimera@bosai.go.jp (H.K.); misumi@bosai.go.jp (R.M.)

* Correspondence: shakti@bosai.go.jp; Tel.: +81-29-863-7502

Received: 29 January 2020; Accepted: 25 March 2020; Published: 1 April 2020

Abstract: During the first week of July 2018, widespread flooding caused extensive damage across several river basins in western Japan. Among the affected basins were the Mabicho district of Kurashiki city in the lower part of the Oda river basin of the Okayama prefecture. An analysis of such a historical flood event can provide useful input for proper water resources management. Therefore, to improve our understanding of the flood inundation profile over the Oda river basin during the period of intense rainfall from 5–8 July 2018, the Rainfall-Runoff-Inundation (RRI) model was used, with radar rainfall data from the Japan Meteorological Agency (JMA) as the input. River geometries—width, depth, and embankments—of the Oda river were generated and applied in the simulation. Our results show that the Mabicho district flooding was due to a backwater effect and bursting embankments along the Oda River. The model setup was then redesigned, taking into account these factors. The simulated maximum flood-affected areas were then compared with data from the Japanese Geospatial Information Authority (GSI), which showed that the maximum flood inundation areas estimated by the RRI model and the GSI flood-affected area matched closely. River geometries were extracted from a high-resolution digital elevation model (DEM), combined with coarser resolution DEM data (global data), and then utilized to perform a hydrological simulation of the Oda river basin under the scenarios of backwater effect and embankment failure. While this approach produced a successful outcome in this study, this is a case study for a single river basin in Japan. However, the fact that these results yielded valid information on the extent of flood inundation over the flood-affected area suggests that such an approach could be applicable to any river basin.

Keywords: extreme rainfall; flooding; river geometries; inundation; digital elevation model; backwater effect; embankment

1. Introduction

Flooding due to extreme rainfall causes loss of life, infrastructure damage, and significant economic loss in many countries every year, making it a major threat to human civilization [1,2]. Unpredictable rainfall behavior over complex urban systems and changing environments may cause an increased risk of flooding. Previous studies have suggested that the frequency of extreme, short duration rainfall events is increasing, such that there may be a higher chance of increased magnitudes and frequencies of flooding [1,3]. Projection reports also suggest that flood frequency may increase, especially over southeast Asia [4,5]. Therefore, understanding the hydrological response to these past events can be a good reference for the proper management of future water-related disasters.

In Japan, torrential rainfall and heavy floods are common and occur during the rainy season. Recently, Japan has experienced extreme rainfall events every year. Based on records and simulation

results of these extreme events, they appear to have increased in number over the last decade [6,7]. One important issue is that severe flooding due to heavy rain is not identical each year. For example, heavy rainfall in 2000 caused heavy flooding in the Tokai district (Aichi prefecture) that exceeded the design levels and complexity of the urban area [8]. Heavy rainfall caused a major flood disaster in Niigata Prefecture on 13 July 2004, which caused levee failures at 11 different locations along six small-to-medium sized rivers, resulting in widespread flood hazards [9]. Extreme rainfall over the Kanto region in 2015 caused heavy flooding across the Kinugawa river basin. Burst embankments along the lower part of the basin caused severe flooding in certain areas of Joso city within the watershed [10]. On 5–6 July 2017, extreme rainfall in numerous basins in northern Kyushu caused serious flooding in many small river basins in mountainous regions. Numerous landslides and erosion also expanded the flood area over these regions [11]. More recently, the event of 5–8 July 2018, caused extensive damage over numerous prefectures in western Japan. Overall, 237 fatalities were reported during this event [12]. The torrential rain triggered widespread flooding in several prefectures, causing property damage and loss of life. Mabicho district within the city of Kurashiki in Okayama prefecture is one of the areas severely affected by flooding during the event. The main reason for such flooding was the collapse of embankments in several parts of the city. The flood killed at least 48 people in the district, submerging approximately 12 km^2 (27%) of the city's land area [13]. Though the types and causes of the flood disasters were not similar in these events, in many cases, flooding was mainly due to the failure of embankments along a river near a settlement area, as in the cases of the Tokai flood (2000), the Joso flood (2015), and the Mabicho flood (2018). Understanding the hydrological processes of these events can allow reduction of the risks associated with their unpredictable nature. Moreover, addressing hydrographic features, such as main tributary embankments in the hydrological analysis, is also important to understanding the possible extent of inundation, especially in urbanized areas.

Hydrological modeling is the fundamental approach for acquiring a detailed understanding of flood processes over any type of river basin. Therefore, several studies have focused on hydrological simulations of flood-affected river basins during extreme rainfall events, focusing on inundation extent [14–19]. Although different types of hydrological models can be adopted in a selected river basin, the most important issue with all of them is to use accurate information during model set up, especially concerning urban river basins. The models' primary input data is rainfall, with several different types of rainfall data available in Japan. Each has specific advantages [10]. Besides rainfall data, the most important input for the model is a detailed overview of the river basin's hydrographic features. This plays a crucial role in flood inundation analysis [20]. Hydrographic information, which can be acquired from different sources, is important for the hydrological models. For example, the Shuttle Elevation Derivatives (HydroSHEDS) is a mapping product [21] that provides hydrological data and maps based on hydrographic information, such as digital elevation models (DEMs), flow accumulations (ACCs), flow direction (DIR), and basin boundaries, which are key datasets used in the hydrological simulation of a river basin [15–17,21,22]. Although several mapping products are globally available, each has their own advantages and disadvantages for hydrological applications [22,23]. Besides DEM data, there are several other important parameters, e.g., meteorological data, ground water parameters, and land use data, that are useful for large-scale hydrological modeling on a long-term basis [24,25]. Previous studies, however, have suggested that the effect of these parameters should be minimal, especially for extreme events [11,18,26].

Different types of hydrological models are globally available. Some models require purchase, while others are open access for research purposes. There is a continuing debate on which model is suitable for the hydrological analysis of a river basin. The selection of a hydrological model depends on the specific interests of the study. Recently, a number of hydrological models have been developed and some of these are available for scientific research, such as HEC-HMS [27], TOPMODEL [28], VIC [29], and DREAM [30].

Each of these models has an extent of physical principle for runoff prediction. For example, HEC-HMS is quasi-distributed or can be used in lumped type, TOPMODEL, VIC, and DREAM

are of semi-distributed type and simulate the hydrologic response of a watershed subject to the hydrometeorological inputs. Some of them can calculate runoff in each grid of a river basin. These models, however, must be combined with a hydraulic model to analyze flood inundation over a river basin [31,32]. The Rainfall-Runoff-Inundation (RRI) model is a two-dimensional, distributed-parameter, structured grid, hydrological model that has the advantage of simultaneously modeling runoff and flood inundation [14]. Several studies have performed flood inundation analysis using global DEMs based on different approaches for river basins from local to global scales [19,22,23,33,34]. In general, different types of global DEM data are freely available for research purposes. HydroSHEDS is an example of this freely available data. HydroSHEDS has been processed and carefully presented for hydrological applications [20,35]. Therefore, it has been used in numerous hydrological modeling studies for specific river basins [15–17,21–23,36]. Information on river geometries, i.e., river width (R_W), river depth (R_D), and embankment height (E_H), are necessary parameters that must be correctly incorporated into the model [36]; these are extracted from DEM data. We note that global data are generally available at a coarser resolution. Extraction of accurate river geometry information, especially for medium-to-small river basins, may yield more uncertainties due to such coarse resolution [22]. In many cases, empirical equations have been used to define river geometries [14–17,19,21–23,33,36–38]. However, obtaining the actual empirical equations of river geometries is a real challenge, particularly for inundation analysis. Therefore, many studies use reference empirical equations [15–17,33,37,38]. The use of high-resolution hydrometeorological and hydrographic data can yield more accurate results when performing hydrological modeling of a river basin. The use of high-resolution data for the hydrological modeling of medium-to-large river basins in a grid format, however, may not be suitable with respect to time constraints and may not be economically feasible. In Japan, several rivers originate from mountainous areas and flow toward flat areas. Therefore, the majority of river basins cover mountains in upstream areas and flat areas along downstream portions of the river basins. Settlement areas along these rivers are common; therefore, a large number of embankment structures have been built along several rivers for flood protection. Both the R_W and R_D parameters within the city area, are often modified and in certain cases, workers have changed the course of the river. Hence, the ability to consider all of these factors is a significant challenge when performing hydrological modeling of any river basin, particularly in Japanese cities.

Gichamo et al. [22] evaluated bias on the vertical cross-section of coarse resolution data, compared to the information from high-resolution DEM data for a limited part of river reach, and agreed that the use of a global DEM is a suitable option, but can produce large uncertainties in flood modeling. Therefore, they recommended that extraction of river cross-sectional data based on a combination of low and high-resolution DEM data could reduce uncertainties, especially for elevation differences along the river channel. Saksena and Merwade [19] also mentioned that the spatial resolution of the DEM data plays an important role in hydraulic modeling. Therefore, they used high-resolution LIDAR data, resampling the DEM data used in flood mapping in their study. Fleischmann et al. [23] considered different spatial DEM scales, i.e., local versus global, to compare river basin inundation profiles. However, they did not obtain significant improvements in their hydrological analyses using local high-resolution DEM data in their analysis. Haque et al. [33] used DEMs from different sources with different spatial resolutions (30–500 m) to simulate discharge, water level, and flood extent, using 2D hydrodynamic modeling. Although they used a high spatial resolution for such a large watershed, the river geometries were based on reference empirical equations. P.C. and Kamimera [37] also used a reference empirical equation to define river geometries and applied it to river basin inundation analysis, but the results were not reliable.

As discussed, direct uses of high-resolution DEM data are not common, especially for medium-to-large river basins. In most cases, DEM data were updated, based on the uncertainties derived from high-resolution DEM data for a limited part of a river, and then directly used in river basin hydrological modeling.

Many challenges remain regarding the proper derivation of river geometries for flood inundation analysis that is based on global DEM data. On the other hand, different types of hydraulic models have been used and several of these models are sufficiently sophisticated, such that they can generate river geometries with DEM data input [18]. However, in other cases, separate river geometries are used in the model to simulate runoff of a given river [15–17,33,37,38]. As previously mentioned, global DEM data may only yield more uncertainties during inundation analysis, such that river geometry extraction based on this data is not feasible. Based on this previous experience, we think that defining river geometries including embankments heights using high-resolution DEM (local) data and adapting these to global DEM data for use during river basin hydrological modeling could be an alternative option which has not been properly tested in previous studies. Therefore, our objective in this study is to produce a rapid hydrological simulation of any flood-affected river basin, using reliable information on river geometries from global hydrographic data, in order to provide a good reference for future extreme events.

In this study, we performed inundation analysis of the flood-affected Oda river basin in Japan during the extreme rain event that occurred from 5–8 July 2018 (Figure 1), using global hydrographic information (HydroSHEDS). We suggest that this analysis, using the RRI model, can produce valid scenarios of the hydrological processes that occurred in the entire river basin. In this paper we discuss the hydrological model in detail and propose a simple concept of river geometry data extraction, which is based on available high-resolution DEM data and Google Earth information. We suggest that merging the extracted river geometry information from a global dataset and adopting it into the hydrological simulations enhances the quality of inundation analysis for any river basin.

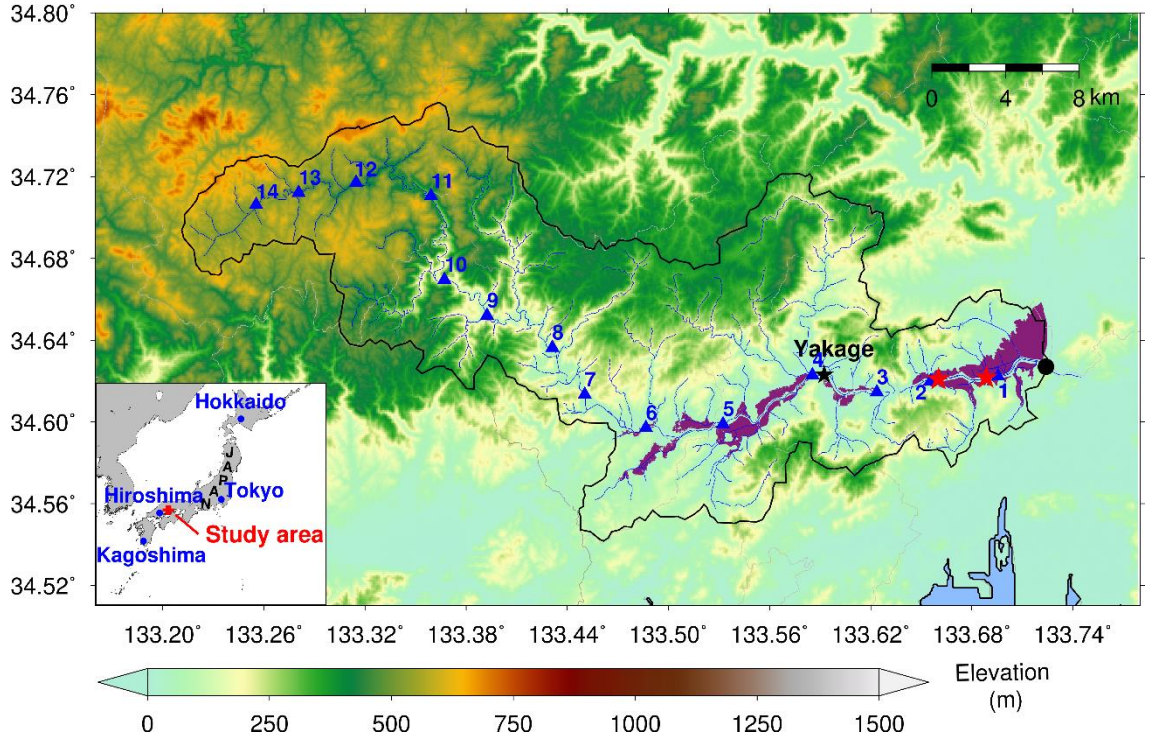

Figure 1. A topographic map showing the location and channel networks of the Oda river basin. Purple shading denotes the estimated flooded area in July 2018 prepared by the Geospatial Information Authority of Japan (GSI). Red stars indicate the failed embankments along the main river channel.

2. Materials and Methods

2.1. Flooding over the Oda River Basin

During the warm season, intense rainfall occurs every year, causing hazardous landslides and floods. In the first week of July 2018, torrential rainfall spanned western Japan.

Typhoon 1807 (Prapiroon) developed over the Pacific Ocean, transporting warm and moist air into Japan's seasonal rain front. Previous storms had produced heavy rainfall in Japan before Typhoon Prapiroon moved through the region. As a result, several prefectures in western Japan experienced the worst impacts of this extreme rain event. Flooding occurred in several river basins, including the Oda river basin (Figure 1). Flooding mainly occurred in the Mabicho district of Kurashiki city (Okayama Prefecture), which is in the lower reaches of the Oda river basin. This region is relatively flat and predominantly covered by urban areas and agricultural fields. A previous study reported that flood waters rose to a depth of 4.8 m in the settlement area of Mabicho district [13].

The Geospatial Information Authority of Japan (GSI) has prepared maps of the areas affected by flooding in the Oda river basin after extreme events (Figure 1). A GSI map of the flood-affected area was compiled from orthogonal images and survey data collected after the event. While this map is an important reference for management purposes, it can also be used to cross-check the results from hydrological simulations. The GSI map shows that the estimated flood area extended to the lower reaches of the Oda river basin. The Oda River is one of the main tributaries of the Takahashi River, which is a major river in Okayama Prefecture. As previously mentioned, heavy rain over the Okayama region generated rises in the water level in the Takahashi River, as well as inhibited flow in the Oda River at the confluence, which caused a backwater effect downstream of the basin and subsequent embankment bursts. The Ministry of Land, Infrastructure, Transport, and Tourism (MLIT) also confirmed riverbank breaches along the Oda river. This river has already experienced several flooding events in the past; flood damage occurred in 1893, 1972, and 1976 along the lower reaches of this river basin [39]. Addressing these issues and delivering accurate hydrological modeling of the flood-prone Oda river basin is an important topic. Therefore, this study focused on understanding a real situation and addresses issues concerning flooding of the Mabicho district in the Oda river basin using the RRI model.

2.2. Datasets

Rainfall information is the main input data in hydrological modeling. We note that rainfall data for the July 2018 event was collected from different sources. The study period was designed from 00:00 JST on 5 July 2018, to 00:00 JST on 8 July 2018. The Automated Meteorological Data Acquisition System (AMeDAS) is a collection of automatic weather stations run by the Japan Meteoroidal Agency (JMA) that perform automatic surface rainfall observations. Similarly, radar rainfall data from the JMA, referred to as analyzed radar rainfall (RADJ), and radar rainfall data from the water and disaster management bureau within the Ministry of Land, Infrastructure, Transport and Tourism (MLIT), were available. Satellite-based rainfall data, i.e., GSMaP, was also available for this event. Recently, remote sensing rainfall data, i.e., mainly satellite-based [16,17,38,40], and weather radar rainfall [10,18,26,32,41] are both quite popular in hydrological modeling, providing a range of options to obtain the most reliable analysis. Estimated rainfall from weather radar observations, however, is characterized by higher spatial resolution for rainfall and can be used for hydrometeorological applications, particularly for specific areas [10,18,26,32,41]. Data for the average basin rainfall in the Oda river basin were obtained and compared using all available rainfall data from the study by P.C. and Kamimera [37]. The radar-estimated rainfall data were quite similar to the measured rainfall data. Moreover, P.C. and Kamimera [37] used all available rainfall data for hydrological simulations of the Oda river basin, determining that simulated hydrological output using radar rainfall data was more realistic and similar to observed data from gauging stations in the Oda river basin. Hence, in this study, RADJ data, with a spatial resolution of 1 km and a temporal resolution of 1 h, were used. JMA provided these radar

rainfall data, which was derived from more than 20 C-band radars distributed across the country, on a real-time operational basis.

Water level data from the gauging station at Yakage were available for this event. These data have an hourly resolution and are available on the water information system of the MLIT website. Using these water level data, the MLIT estimates the discharge data at the station and posts the levels on their website for public use. Unfortunately, no discharge data were reported for 2018 using the water level data from that station.

Hence, we first collected the discharge and water level data for the months of July and August for the three previous years. Then, an empirical equation was fitted to the water level and discharge based on the collected data.

Global hydrographic data from HydroSHEDS, which provides hydrographic information in a consistent and comprehensive format for regional and global-scale application in different spatial resolution format, was used. In this study, the 3″ resolution of HydroSHEDS was downloaded (https://hydrosheds.cr.usgs.gov), which is freely available for research purposes. HydroSHEDS includes ACC, DIR, and DEM data. It includes hydrologically conditioned DEM, and therefore, is suitable for hydrological applications. Data from Google Earth, specifically the elevation profile, is also used in this study.

High-resolution DEM data (5 m spatial resolution), concerning the development of river geometries of Oda river, were also collected from the GSI webpage (http://maps.gsi.go.jp); these are also freely available for research purposes. According to GSI, the standard deviation of the difference between actual and estimated heights is 0.3 m or less in a grid cell containing lidar measurements (2 m or less in a grid cell, not containing the measurements). Moreover, as discussed in the previous section, GSI maps of flood-affected areas were also downloaded from GSI.

2.3. RRI Model

In this study, we aim to properly define river geometries and use them to perform rainfall-runoff modeling of the urbanized river basin. Moreover, our target is to perform inundation analysis of a river basin. Therefore, considering such issues, we require a model that can compute the runoff and inundation profile over a river basin. The hydrological response in each grid of the river basin is also of interest in this study.

The RRI has the advantage of simultaneously modeling runoff and flood inundation. Therefore, we used the RRI model in this study. The RRI model calculates the hydrological response in a grid cell at the location of a river channel. The model assumes that both the slope and river are positioned within the same grid cell. The channel is discretized as a single line along the centerline of the overlying slope grid cell. Detailed mathematical explanations of the RRI model are reported in several previous studies [14–17,38,42]. The detailed outline and technical references of the model are provided in the RRI user manual [43]. Additional studies have applied this model to simulate the flooding of various river basins [15,16,21,37].

The flow on the slope grid cells is calculated with the 2D diffusive wave model. For the river routing model, a 1-D wave diffusive wave model is applied to river grid cells. River geometry, i.e., river width (R_W), depth (R_D), and embankment height (E_H) must be defined during model set up. If detailed information on river geometry is not available, R_W and R_D can be approximated [14] based on the following functions with respect to the upstream contributing area, A (km^2):

$$R_W = C_W \times A^{S_W} \quad (1)$$

$$R_D = C_D \times A^{S_D} \quad (2)$$

where C_W, S_W, C_D, and S_D are unit-less constant parameters. They can be generated based on the relationship between their respective geometry (R_W or R_D) and contributing area (A). The model [14] defines default parameters, which may be applicable for a mountainous river basin. The model

considers the cross-section profile of a river as a rectangle. For embankment settings, E_H can be fitted in two ways. The first one is by considering the height along the river, such that E_H can be set to a height of > 0 for a river whose width is > 0. In this option, E_H should be identical on both river banks. The second option is that we can fix E_H wherever the exact embankments are located and obtain a separate file that can be used in the model.

2.3.1. Extraction of River Geometry Data

Numerous studies have discussed the empirical equation to develop river geometries e.g., [33,44]. Of course, the empirical equation can be considered using references as the basis, but this can lead to more uncertainties for the hydrological outputs. In this study, we propose a simple approach to generate R_W, R_D, and $E_{H,}$ based on high-resolution DEM data (5 m), Google Earth information, and existing river networks. Hence, to extract the empirical equation for river geometries, we followed the following procedures: First, we selected random points over the main Oda river basin (Figure 1). River geometries, i.e., R_W and R_D, for all the selected points were obtained. Similarly, the basin area for those points was also calculated and finally, the area of the selected point vs river geometries was carefully analyzed. From these data, the empirical equations were fitted and can be applied for the whole river basin.

We believe that this methodology of obtaining river geometries is beneficial for application purposes. However, we did not apply the same process to the tributaries of the Oda river, which is one of the limitations in this study. We suggest that sampling at certain points can be used to represent the entire basin and does not yield significant differences on the extent of inundation, especially over the lower reaches of the basin.

For E_H, we mainly focused on the major river in the basin, up to a certain distance. Considering the river channel networks from the 5 m DEM data, we can extract the maximum height along the selected river. Similarly, corresponding points were extracted some distance from the maximum heights. We note that the selected locations at points along the left and right banks follow a straight line that should be perpendicular to the center line of the river. This procedure was repeated several times at specific intervals from the outlet of the basin to a certain distance in the river basin. Then, based on the trend of these selected points, we can fit an empirical equation.

2.3.2. Model Set up

Hydrographic features: ACC, DIR, and DEM data must be fixed for the Oda river basin to set up the model. We downloaded these data from HydroSHEDS, which was developed based on the SRTM3 DEM [35], and rearranged the data for the Oda river basin. We separately used the 3″ HydroSHEDS data for the river basin. Next, we used the default empirical equation to set R_W and R_D over the river basin while we fixed E_H at a zero height to all the rivers of the basin. This was the preliminary model set up for the river basin. P.C. and Kamimera [37] have reported detailed simulated procedures and results obtained from such a preliminary model set up. In this study, we use new river geometry empirical equations in the model.

Rainfall is key primary data for hydrological simulations. P.C. and Kamimera [37] discuss the rainfall data and spatial resolution of the HydroSHEDS data in detail. They used all available rainfall data and separately performed hydrological simulations of the Oda river basin using different hydrographic data types. They confirmed that the use of the 3″ resolution hydrographic data, with radar-estimated rainfall data, produces a more reliable simulation. Therefore, based on their preliminary analysis, we used the 3″ hydrographic and RADJ data to set up the model. Moreover, P.C. and Kamimera [37] suggested that accurate information on river geometries for the model set up can allow us to understand the real situations concerning inundated flooding over the river basin.

The RRI model properties are highly sophisticated and certain parameters can be tuned [14,17]. In this study, however, we compared simulation results by applying the best reference parameters. If a model result appeared at a satisfactory level, we did not change any model parameters. To compare

the modeled and observed results for the Oda river basin, we considered several statistical tools, i.e., the Nash-Sutcliffe efficiency (NSE), the root mean square error (RMSE), the mean absolute error (MSE). Mathematical explanations for these tools are reported in several previous studies, e.g., P.C. et al. [26]. We also used the Kling-Gupta efficiency (KGE, [45]), which is based on mean, standard deviation, and correlation of observed and simulated data.

3. Results

One of the main objectives of this study was to conduct flood inundation analysis over the Oda river basin. In such a case, river geometries are important and must be correctly incorporated into the model. In a previous study done by P.C. and Kamimera [37], default empirical equations were used to generate R_W and R_D with no embankments, with clear indications that river geometry reconstruction is necessary to obtain correct information on flood inundation over the basin. Therefore, obtaining appropriate empirical equations for the river geometries within the river basin is the first priority.

3.1. River Geometry Profiles

We note that the 3″ DEM data from HydroSHEDS has a spatial resolution of approximately 90 m. Using this DEM data, we cannot extract actual R_W, R_D, and E_H profiles due to its coarser resolution. Our objective in this study was to fit empirical equations for R_W, R_D, and E_H for the major river within the basin. To do this, we considered high-resolution DEM data with a spatial resolution of 5 m and Google Earth images. We note that the 5 m DEM data are available for certain regions of Japan, which can be downloaded for free. For the upper reaches of the Oda river basin, a 5 m DEM is not available. We, therefore considered elevation profiles from Google Earth to estimate the R_W and R_D profiles. Google Earth includes an elevation profile tool that provides elevation details at any chosen point along a path. We simply selected each of the 14 points in Figure 1 to obtain details of the river geometries. The river cross-section profile from DEM data was obtained from the 3D analyst tool of ArcGIS. The estimation of R_W appears to be similar to the width extracted from the 5 m DEM along the lower reaches of the Oda river basin, but we did not find the same case for R_D. We note that R_D is more useful than Rw and decided to obtain it from Google Earth, in the absence of a high-resolution DEM. We also observed that using information from Google Earth, especially in the upper reaches of the basin, does not affect the flood inundation analysis. We do not discuss the quality of the high-resolution DEM and HydroSHED data because this is beyond the scope of our study.

3.1.1. River Width (R_W)

First, cross-sectional profiles of the Oda River were generated at several selected points (i.e., blue triangles in Figure 1) using the 5 m DEM data. For example, Figure 2 shows a cross-section profile at the lowest point in the basin. Based on the cross-sectional profile of the Oda river for that point, we can appropriately estimate the R_W of the river at that point. Similarly, we can estimate the river basin area (A) for that point. These procedures were applied to the other selected points along the Oda river. As the 5 m DEM data is not available over the mountainous parts of the basin (upstream of the Oda river), R_W was extracted from Google Earth elevation profiles. After calculating the corresponding basin area for all points, we prepared the R_W-A relationship for the Oda river (Figure 3). The default R_W-A relationship based on the RRI model appears to be different when compared with the fitted R_W-A relationship for the Oda River, especially in the lower reaches of the river basin. There are, however, several similarities, particularly in the upper reaches of the river. Hence, we can fit the empirical equation we developed to the Oda River, whose basin area is greater than 110 km^2. The default empirical equation in the RRI model was used for entire rivers and their tributaries whose basin areas were lower than 110 km^2 in this study (Figure 3). The default reference empirical equation for the RRI model is suitable for a mountainous river basin [43]. It is clear that R_W of the Oda river is large as compared with the default width at the lower part of the basin. Such scenarios could be

attributed to human encroachment of river width around the urban area. However, R_W values were found to be similar over the upper part (mountainous areas) of the basin.

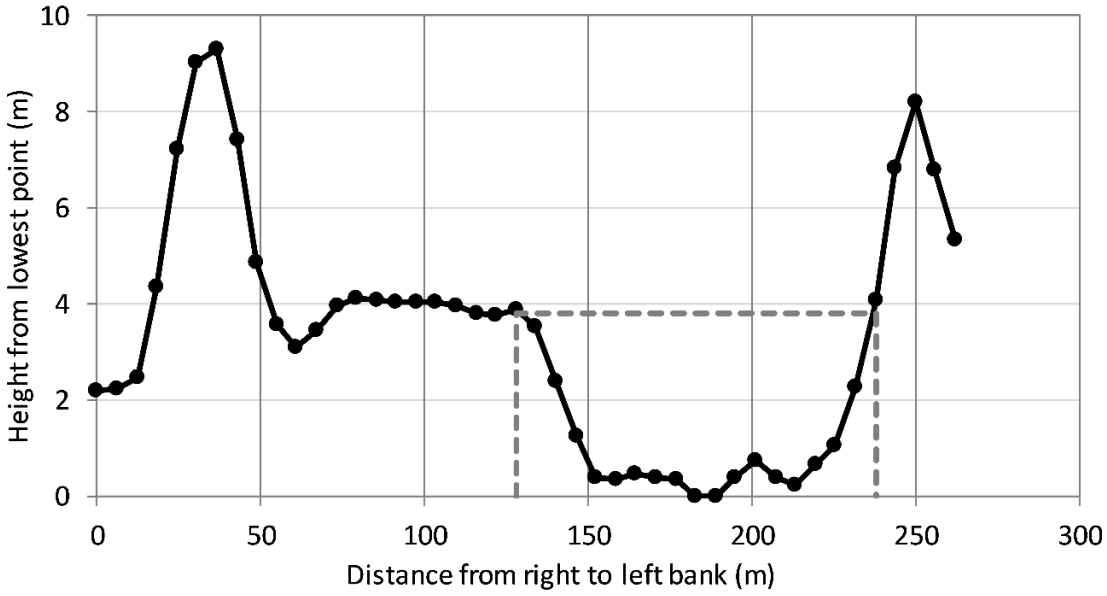

Figure 2. River cross-sectional profile at a point across the Oda river basin. The gray dotted line indicates the river width and depth profile at this point.

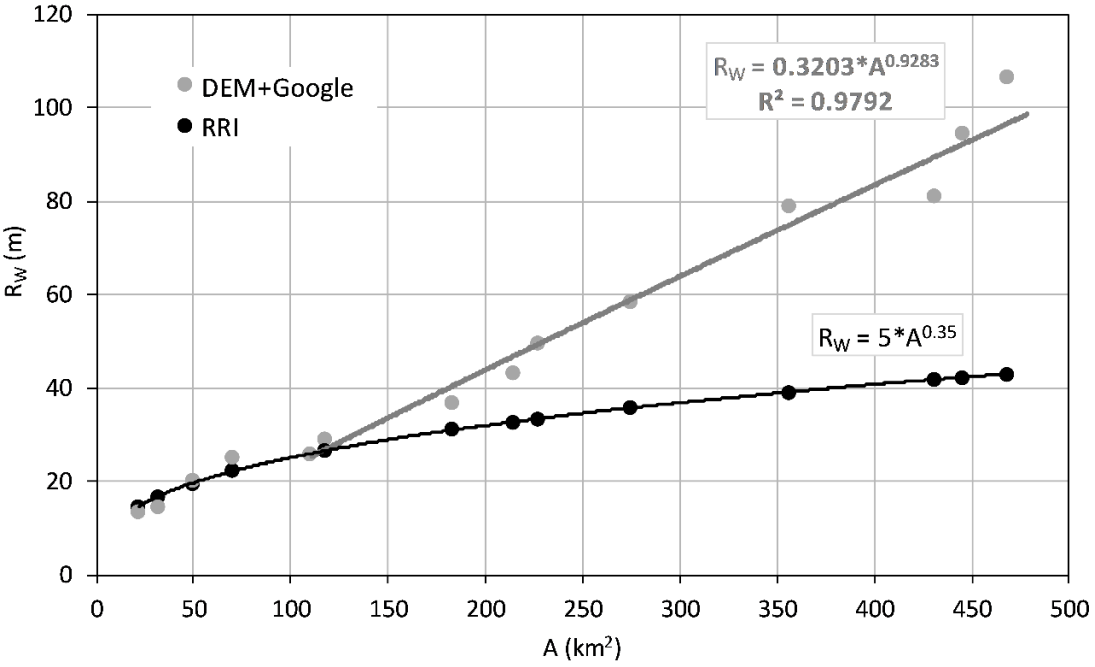

Figure 3. The relationship between the river basin area (A) and river width (Rw) for the Oda river basin. Black and gray points with fitted black and gray lines indicate the default Rw-A relationship based on the Rainfall-Runoff-Inundation (RRI) model and digital elevation model (DEM)/Google Earth data, respectively.

3.1.2. River Depth (R_D)

Obtaining accurate R_D information is a challenge currently faced by the hydrological community. To generate the R_D profile of the Oda river, we followed the identical procedure used for R_W in the first step.

After creating a cross-section profile of any point along the river (Figure 2), we obtained the depth from the difference between the lowest point of the river cross-section and the surface height of the selected R_W. Figure 4 shows the R_D-A relationship of the fitted and default RRI model. The maximum R_D at the most downstream section of the Oda river was approximately 4 m. This value significantly fluctuated within a short distance from the outlet of the basin.

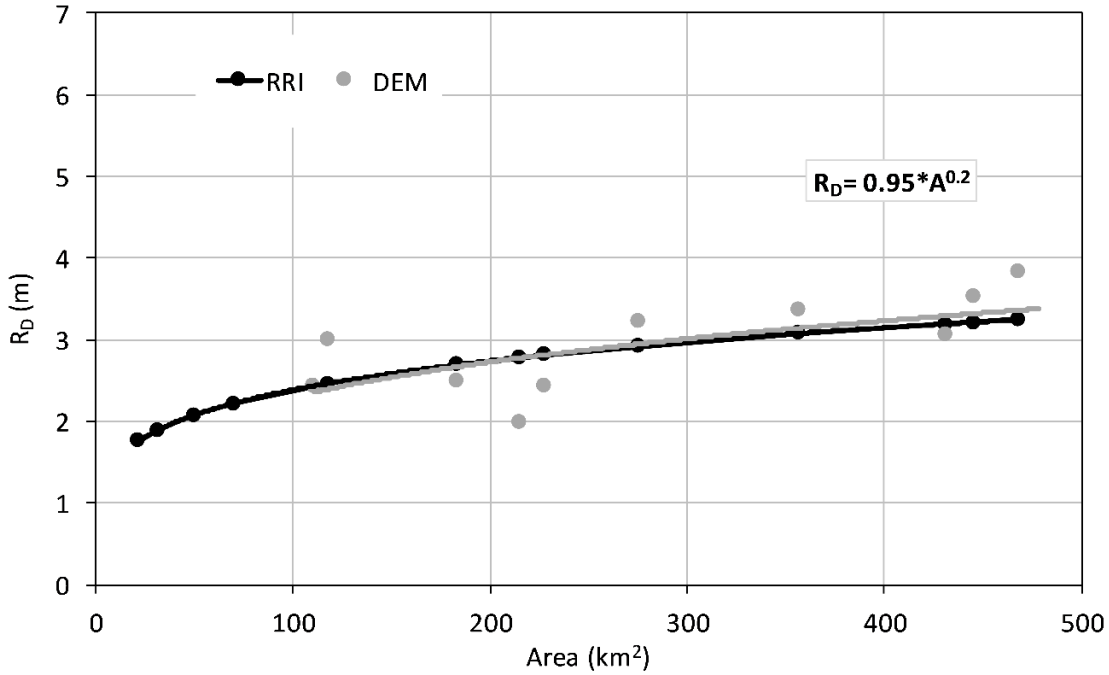

Figure 4. The relationship between the river basin area (A) and river depth (R_D) for the Oda river basin. Black and gray points with fitted black and gray lines indicate the default R_D-A relationship based on the RRI model and DEM data, respectively.

Overall, trends in R_D-A relationship fluctuated slightly more than trends in the R_W-A relationship for the Oda river. We fitted the empirical line, which was similar to the default equation of the RRI model. Therefore, we used the default empirical equation during simulation.

3.1.3. Embankment Height (E_H)

Man-made embankments are common along rivers in Japan. There are numerous embankments along both sides of the Oda river and its tributaries, particularly in the Mabicho district. It is hard to observe embankments on coarse DEM data. We note that 3" hydrography datasets were used during model setup. Therefore, we also used the 5 m DEM to retrieve the embankment heights along the Oda river. In this study, we attempted to extract the E_H to only a few kilometers of the basin's major river. Exclusion of embankments along the major river's tributaries is a limitation of this study.

Maximum peak heights along both banks of the river and their corresponding heights for the adjacent peak points (i.e., approximately 50 m from the peak points) were extracted. We note that nearby points were not considered in the river's cross-sectional area. Hence, we subtracted corresponding points from the peak point along the Oda river for both banks, which is shown in Figure 5. We can observe that E_H values along the left bank are higher than those along the right bank. We note that settlement areas and agricultural land along the left bank of the river occupy a larger area than along the right bank. We found a linear trend between the E_H and distance from the outlets. However, we observed numerous fluctuations in the E_H. Point selection and their heights can take buildings, bridges, and tributary dikes into account, which are all structures that can create fluctuations in E_H along the distance of the river.

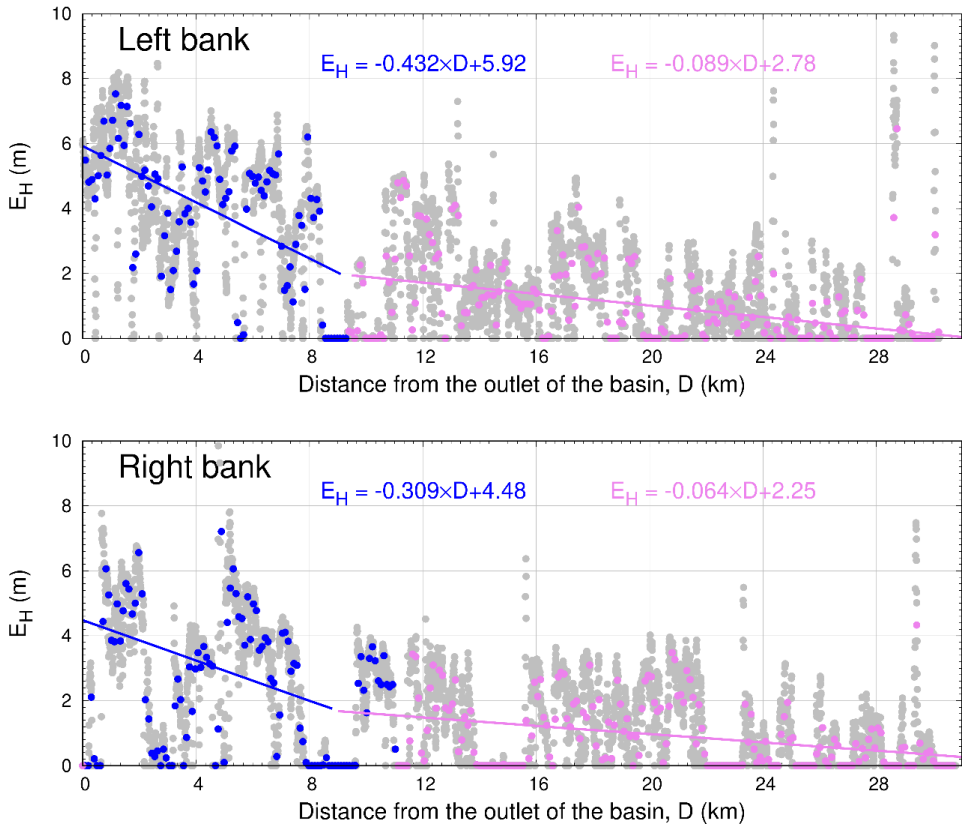

Figure 5. Embankment heights along the main river in the basin. Fitted lines were drawn by considering a moving average of 20 points in the original datasets.

Based on the E_H-D relationship, we fitted the linear trend line for both banks (Figure 5). There were two linear trends for both banks. A poor trend appeared from the outlet of the bank up to approximately 9 km, after which there was a slight flattening of the slope observed for the same bank. Four different types of trends were generated for the left and right banks of the river, up to approximately 30 km from the outlet of the river basin. The fitted E_H-D relationship for up to 9 km and greater than 9 km from the outlet of the basin (D) were $E_H = -0.432 \times D + 5.92$ and $E_H = -0.089 \times D + 2.78$, respectively, while the left and right banks, were $E_H = -0.309 \times D + 4.48$ and $E_H = -0.064 \times D + 2.25$, respectively. It is noted that the E_H profile along Oda river is clearly visible and such relationships (R_W-A, R_D-A, and E_H-D) would vary in every river; this should be addressed in the model set up of RRI.

3.2. Hydrological Simulation

After incorporating new river geometries for the Oda river, all of the information discussed previously was used for a second model setup. Then, hydrological simulation was performed for the period from 00:00 JST on 5 July 2018, to 00:00 JST on 8 July 2018. Three major components, i.e., river water discharge, river water level, and inundation depth, were simulated at each grid of the river basin. To evaluate model performance, we compared the results of our simulations with observed and estimated data from the Yakage hydrological station (Figure 1) located in the basin. The relationship between the observed and simulated discharge at the Yakage station is shown in Figure 6, and similarly, Figure 7 shows the water level for that station.

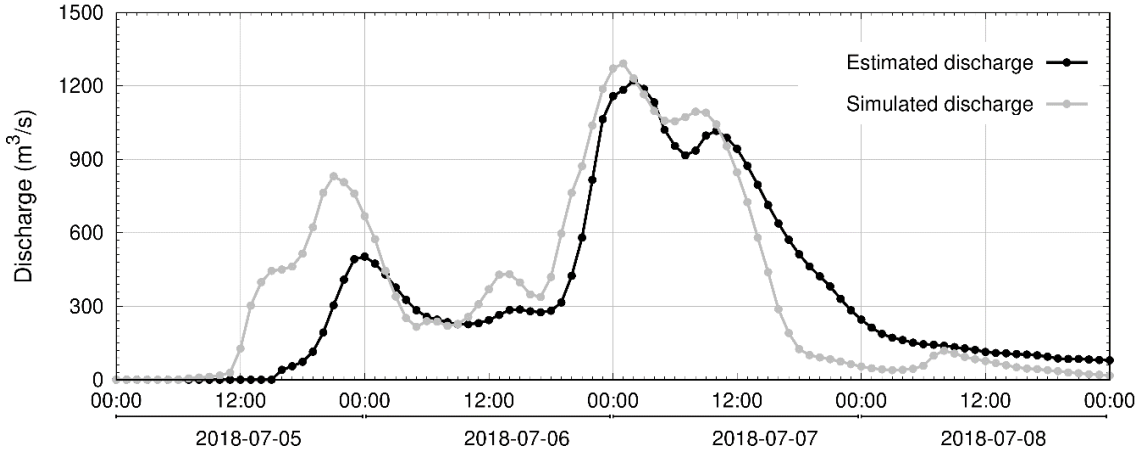

Figure 6. A time series profile of the discharge at the Yakage station in the Oda river basin.

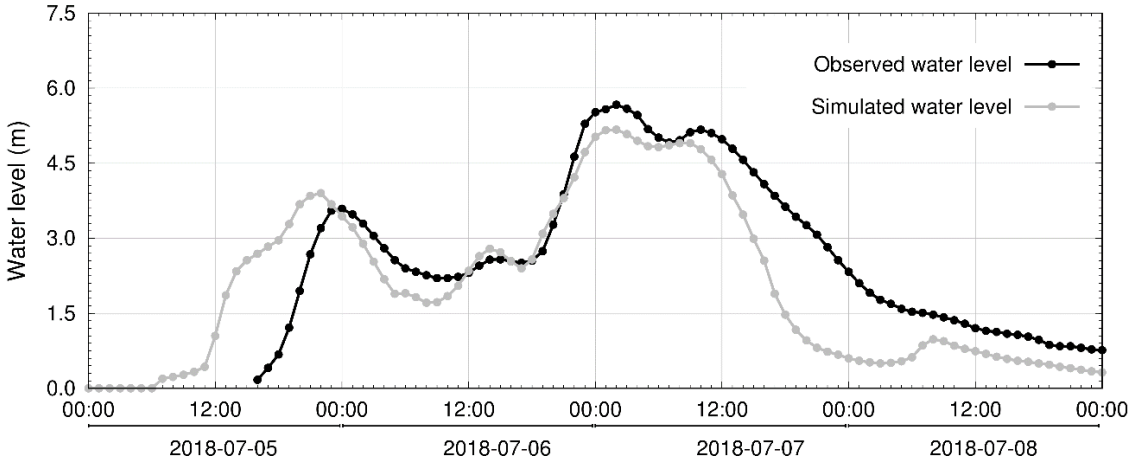

Figure 7. A time series profile of the water level at the Yakage station in the Oda river basin.

The values of the Nash-Sutcliffe efficiency (NSE), Kling–Gupta efficiency (KGE), root mean square error (RMSE), peak difference (PD), and mean absolute error (MSE) for the observed and simulated water levels were 0.73, 0.78, 1.02, 0.50, and 0.75 m, respectively, while for discharge the values were 0.70, 0.82, 184.45, −9.44 m^3/s, and 114.70 m^3/s, respectively. We note that the simulated peak value of the water level was slightly underestimated while discharge for that point was slightly overestimated.

We suggest that such scenarios are acceptable. Overall, these statistical assessments indicate that model performance was similar for the event analyzed here; we suggest that there is no need to calibrate the model parameters for this river basin. From the RRI simulation, we obtained three outputs at each grid scale of the basin—discharge, water level, and inundation profile. Based on the statistical assessment, we confirmed that adaptation of the RRI model utilizing global hydrographic information, performed well in the estimation of discharge rate as well as the water level of Oda river. We can also confirm that the estimated river geometries for the Oda river are acceptable for further inundation analysis over the basin.

3.3. Flood Inundation Analysis

One of the most important pieces of information from hydrological simulations is the inundation depth over the basin. Figure 8 shows the maximum flood inundation depth profiles in the river basins during the rain event. The maximum inundation depth varied significantly among the basins, i.e., a maximum modelled inundation depth of 5.5 m. Inundation areas were not only in the lower reaches of the basin's major river, but also extended to upstream and to minor rivers and small tributaries.

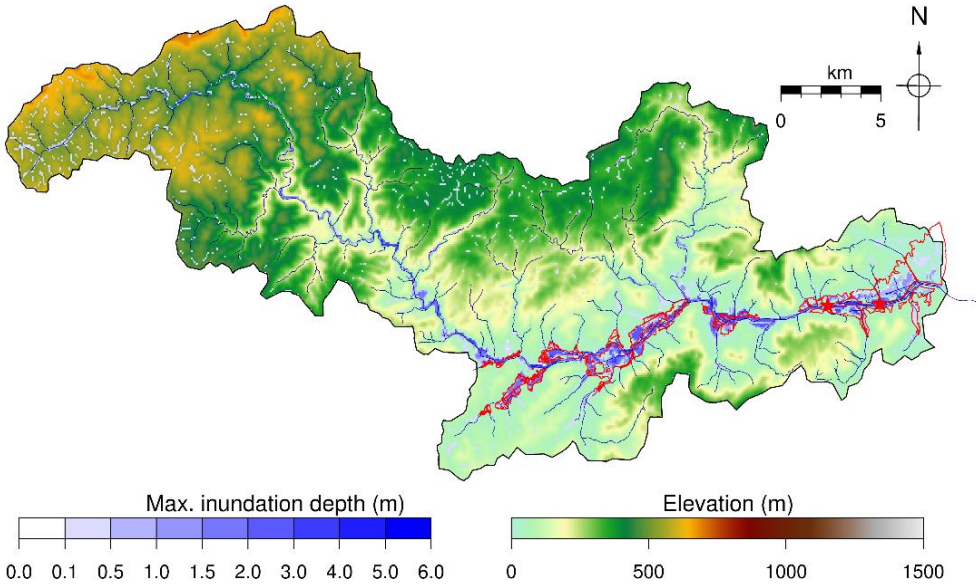

Figure 8. The maximum inundation flood depth profile over the Oda river basin. Red polygons are the estimated flood inundated area based on the GSI maps.

A GSI map of the flood-affected area was compiled from orthogonal images and survey data collected after the extreme rain event of 5–8 July 2018 (see the red polygon in Figure 8). We overlaid the GSI map on the modelled flood inundation map and found that, in most cases, the two data sets did not have a good relationship, particularly in the lower reaches of the basin; however, the upper part of the GSI map and the simulated inundation profile show a close match. We considered the continuous embankments along the basin's major river except for certain major tributaries. Such continuous embankments along the main river can block the flow in small tributaries near their confluence with the main river, which reflected a slightly wide coverage of inundation depths along the basin's major river. But it should be noted that we did not use the embankments' heights at the confluences of the main river and the large tributaries.

In the absence of river embankments, the simulated results showed a close match between the estimated and modelled maximum inundated area over the lower reaches of the basin, which was, in fact, not the real situation that occurred in the Oda river basin [37]. In this study, however, we did not obtain evidence of flood inundation over the Mabicho district after updating the river geometries. We note that the simulated results performed well at the Yakage station (Figure 1), which is the upper boundary of the Mabicho area in the basin. We can confirm, however, that the hydrological simulations of the Oda river basin did not reflect flood inundation, particularly over the Mabicho district, based on the conditions that were adopted in this study. Therefore, we suggest that further scenarios should be considered in the model to address the flood inundation situation over the Mabicho area of the basin.

3.4. Flood Event Scenarios

There were several discussions about the flooding situation in the Mabicho district area after the event occurred in July 2018. The first important point is the bursting of embankments that occurred [13,39]. Field survey documents prepared by the MLIT contain evidence of these bursting events [46]. Figure 1 indicates the broken points along the Oda river in the district. Another significant issue was the backwater effect, which has been briefly discussed for this case [13]. Based on the report of Maininchi, Japan [13], the water level rose over the Takahashi river, which is the main river in this region. Then, downstream flow of the Oda river was trapped with rising water levels in the Takahashi river. Stagnant flow further increased the water level until the point of embankment breaching and flood occurrence. Profs. Shiro Maeno (Okayama University, Okayama, Japan) and Masato Sekine

(Waseda University, Tokyo, Japan) were interviewed in this report. They both agreed on the occurrence of a backwater effect in the Oda river basin, mentioning that such scenarios could occur anywhere across the country during future extreme rain events [13].

Based on the backwater effect and the failure of embankments in the Oda river basin, we reconstructed the model for the Oda river basin. Flow in the Oda river should have increased simultaneously with the Takahasi river. If flow from the Takahasi river attempted to enter the Oda river in the opposite direction, high water velocities at the outlet of the Oda river should not allow a significant amount of water to enter into the flow of the Takahasi river. Instead, we suggest that flowing water in the Oda river was blocked at the outlet of the basin due to increasing water levels in the Takahasi river. Therefore, our first assumption was to set the embankment height to zero at the two points on the left bank of the river in the elevated DEM (see the star points in Figure 1), such that the embankment can be equally divided. The second assumption was to trap flowing water at the outlet of the basin to initiate the backwater effect. To do this, we elevated the cross-section profile at the outlet of the basin so that flow water in the Oda river cannot enter the Takahashi river, which initiated reverse flow. Obtaining the depth of the water level at the bank of confluence along the Takahashi river is difficult, and therefore, we assumed a simple approach. For example, the river depth downstream of the river basin was approximately 4 m and embankment height at left bank was approximately 6 m. It is important to note that there was no overflow of flood water from the embankments at that point. We checked the maximum simulated water level height at that point during the first simulation results and found that maximum water level height was approximately 5 m. We estimated that a water level of less than 5 m would not allow the overflow of flood water from the embankments. Hence, we elevated the DEM data by 4 m at the outlet of the basin to ensure backwater effect. In reality, however, obtaining the actual height is difficult.

The exact time at which the backwater phenomenon and embankment bursting occurred is vital information. The MLIT sent an emergency email concerning the overflow of the Oda river along the right bank in the Mabicho district at 00:47 JST 7 July 2018. The MLIT also confirmed bank breaching along the Oda river several hours later [13]. We note that the maximum peak water level was observed around 00:00 JST on 7 July 2018, at the Yakage station (Figure 7). Hence, we can assume that continuous increases in the water level must have occurred earlier than 00:00 JST on 7 July 2018, which indicates that the backwater phenomenon begun earlier. The exact timing of the bursting river embankment, however, is difficult to understand in such a disaster event. In the model setup, the failure of embankments and backwater effects were fixed within the entire simulation time period. Using this information is not favorable for simulations after a certain period or by varying the model.

We then used the model to simulate the Oda river basin a second time. Figure 9 shows the maximum inundation profile over the Oda river basin. The maximum inundation depth along the upper reaches of the basin is nearly identical to the maximum inundation depths shown in Figure 8. There are, however, several differences in the lower reaches of the basin.

The simulated flood area showed a good relationship with the estimated flood inundated area based on the GSI map. Certain areas of the basin were not covered by inundated water. This could be due to several reasons, i.e., DEM data quality, the actual magnitude of the backwater effect, or effects from minor river flow and their embankments. Overall, adding the flood scenarios option in the model, we obtained a reliable simulated flood inundation profile over the Oda river basin for the extreme rain event of July 2018.

To understand the extent of flooding over the Mabicho district, we performed time series profiles of the maximum flood inundation profile over the district (Figure 10). Three different time periods, i.e., 23:00 JST on 5 July, 14:00 JST on 6 July, and 12:00 JST on 7 July (2018), were selected to observe the maximum simulated flood inundation profile.

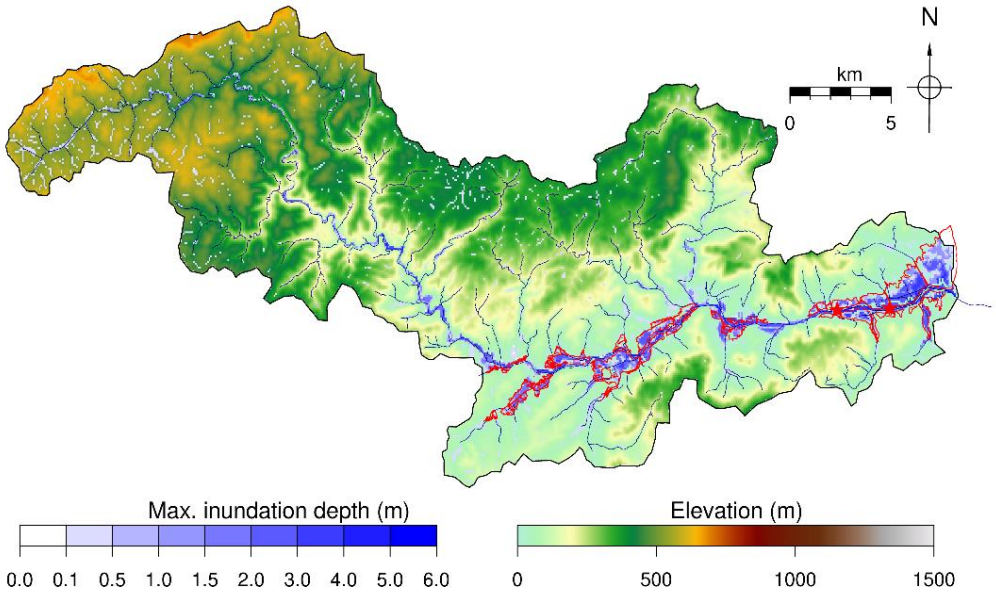

Figure 9. The maximum inundation flood depth profile over the Oda river basin that takes into account embankment bursting and the backwater effect. Red polygons are the estimated flood-inundated area based on GSI maps.

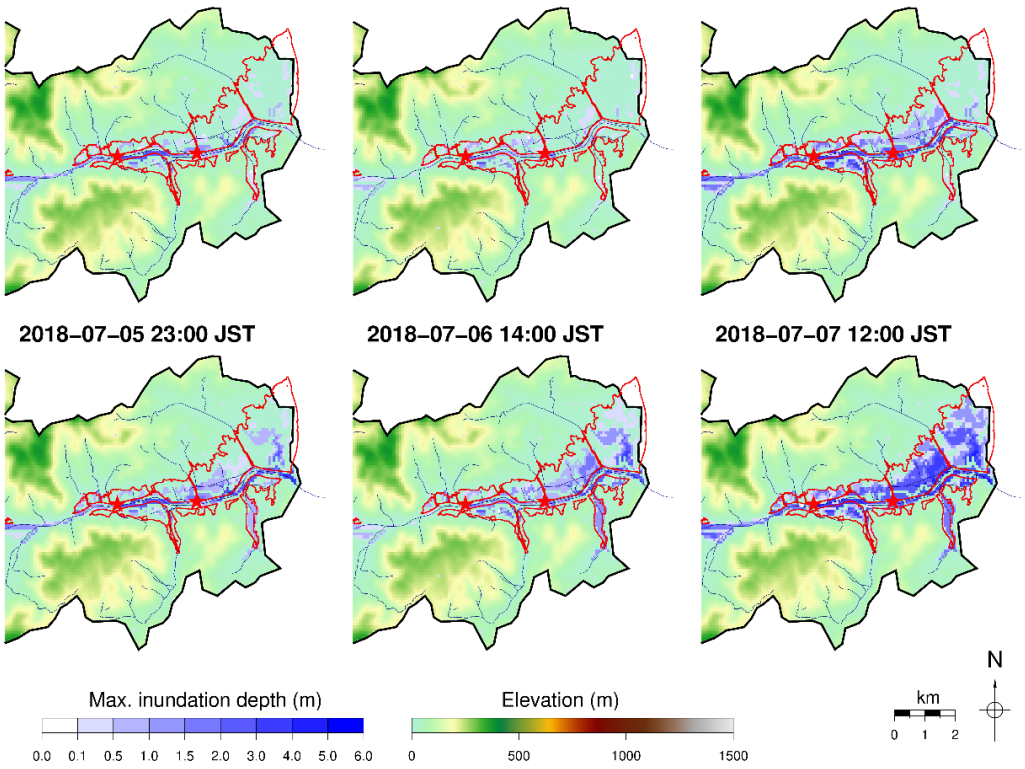

Figure 10. Simulated maximum inundation depth profiles over the Mabicho district in Kurashaki city (Okayama prefecture) during different periods. The upper profiles indicate normal conditions while the bottom panels show the effects of the back-water phenomenon and embankment bursting along the Oda river. Red polygons indicate the estimated flood area based on the GSI maps.

We were unable to obtain an inundation profile without considering the backwater and embankment failure effects in the Oda river (Upper panel of Figure 10). When considering these effects, we observe that flooding appeared after 14:00 JST on 6 July 2018, in the Mabicho district (Lower panel

of Figure 10). Therefore, the scenarios that were considered in the model and the actual flooding situation for the Oda river, based on the MLIT, match.

4. Discussion

Different types of radar have been used to record, monitor, and forecast precipitation in Japan for operational and research purposes. However, each type of radar rainfall data have their merits and demerits [10]. In this study, we used radar rainfall data with spatial resolution of 1 km, which is the optimal spatial resolution of radar rainfall data for the hydrological modeling of a river basin for such extreme event [26]. MLIT established an eXtended RAdar Information Network (XRAIN) that uses an operational data processing system developed by the National Research Institute for Earth Science and Disaster Resilience (NIED; [47]). XRAIN consists of X-band multi-parameter radars and has spatial and temporal resolutions of 250 m and 1 min, respectively. Selection of proper temporal resolution of radar rainfall data could be another good topic for hydrological applications; however, consideration of the fixed temporal resolution of each rain event is one of the limitations of this study.

Global hydrography data (HydroSHEDS) with 3" (approximately 90 m at the equator) spatial resolution were used in the model, which is one of the available global high-resolution scale hydrography maps. A substantial amount of manual labor has been performed to ensure quality control of HydroSHEDS [20]. However, recent studies [48] have pointed out that there are possible uncertainties associated with these data. In this study, we did not analyze the uncertainties associated with HydroSHEDS and also did not include other global DEM data for this basin, which was beyond the scope of this study. As several global DEM datasets have been released for research purposes [48,49], finding the best global DEM dataset for a river basin in a specific area/region is a possible topic for future studies.

Therefore, several studies have discussed the optimal scales for DEM and hydrometeorological input data [26,50]. However, if we desire rapid hydrological simulations on a nearly real-time basis, the direct use of high-resolution DEM data to model a large river basin may not be suitable.

The long computational time required is questionable in terms of cost benefit analysis. Therefore, these factors have posed challenges to conduct prompt inundation analysis within a river basin. Hence, one of the key points in this study is our ability to obtain all required information using the resources available within the global datasets (coarser hydrography data) to rapidly simulate the extent of inundation. Hence, we used high-resolution DEM data to develop river geometries of the Oda river basin. Very high-resolution DEM data (5 m) were also used in this study. It should be noted that the land use profile of the river basin has been changing due to human encroachment and urbanization, Therefore, there could uncertainties in the high-resolution DEM data. Use of updated DEM data is recommended, if available.

The generation of river geometries, especially R_W and R_D, is a classical process [44]. Although the empirical equations for river geometries appear to vary for a selected river in a specific study [15,16,21,44], in certain cases, empirical equations were used based on reference data [15–17,33,37,38]. In this study, we generated river geometries based on the observation of certain points along the Oda river, which indicated that accurate river geometry information should be obtained before hydrological simulation of that river basin. More points can be selected, but the fitted empirical lines were sufficient for the 14 selected points. This is an example where select limited points can also yield a sufficient empirical equation of the river geometries in a river basin. Despite the absence of high-resolution DEMs, we can, at least, obtain field observations for these 14 points within a river basin, which can be used to generate empirical equations, especially for R_W and R_D. Such scenarios are beneficial for basins that do not have high-resolution DEM data available.

We understood that there are several tributaries inside the river basin and that not locating data points in those tributaries might have introduced some uncertainties. However, our main concern goes to the main river channel in the basin, so that the lack of data from all of the river networks in the basin does not lead to significant error, at least for the hydrological output of the main river in the basin.

Similarly, extracting an empirical equation for embankments was only limited up to the major river inside the basin. Indeed, man-made embankments can be applied to the small river tributaries, especially in the city area. What we believe, though, is that severe flooding and embankment failures in a major river can easily obscure any flooding in the small tributaries with embankments. In this study, an empirical equation representing river embankments was used in the model. Such empirical equations may have certain uncertainties because of fluctuation points around the trend line; hence, the use of extracted points at each pixel distance could be an alternative option for application in the model. Naturally, trends in river geometries for any river basin may differ from that obtained in this study.

After obtaining reliable river geometry information for the Oda river, we used this data to set up the model for the simulations. Model performance and the simulated results were evaluated with observation datasets. We found that the simulated and observed hydrological outputs, water level, and discharge followed identical trends. It should be noted that only rainfall data was used in the RRI model as a meteorological parameter for this flood event. This was an extreme event and hence, we excluded other meteorological parameters that may cause certain uncertainties, specifically at the initial simulation phase.

To address the real characteristics of flooding scenarios, the model setup was redesigned for this specific event. This included two main changes, i.e., embankment bursting and a backwater effect in the Oda river, that were inserted into the model to perform a second simulation of the river basin. The area of the maximum simulated depth was then verified with the estimated flood area based on GSI maps for the Mabicho region. The RRI model does not include inputs regarding embankment failure and backwater effects. We included those effects, based on a simple assumption that such an approach should be incorporated in any hydrological model to accurately understand the flood scenarios in a river basin. However, we agree that this simple approach may have some limitations. For example, in the model setup, we considered that the scenarios (i.e., time of embankment collapse and backwater effect initiation) were fixed from the beginning of the simulation. Considerations of the exact time and total duration of these scenarios were not possible in the model.

Flexibility with respect to the adoption of scenarios at specific times during the entire simulation period is an important issue for future model development.

5. Conclusions

Torrential rain caused heavy flooding from 5–8 July 2018 over the Oda river basin, which caused severe flood inundation in the Mabicho region and lower parts of the basin, significant loss of life, and severe infrastructure damage. For these reasons, a detailed understanding of flood processes is necessary for the proper management of water resources in the basin. Therefore, this study attempted to analyze inundation over this basin using the RRI model.

Information on river geometries plays a significant role for the hydrological response of the simulation to more closely match with reality. We first retrieved accurate river geometry information before performing hydrological simulations of the river basin. Empirical equations for the river geometries, i.e., R_W, R_D, and E_H, of the Oda river were developed in this study. We suggest that such a methodology can be highly useful for basins where high-resolution data are not available. The basic principles of this model can be used to easily generate river geometries, and we suggest that this method can be applied to global river systems.

After obtaining reliable river geometry information for the Oda river, we used this data to set up the model for the simulations. Model performance and the simulated results were evaluated with the observation datasets. We found that the simulated and observed hydrological outputs, water level, and discharge followed identical trends.

Flood inundation was then analyzed over the basin, showing that the simulated flooding extent did not correctly match the extent observed over the Mabicho district (i.e., the downstream section of the Oda river basin). To address the real characteristics of flooding scenarios in the Mabicho district, the model setup was redesigned for this specific event. This included two main changes, i.e.,

embankment bursting and a backwater effect in the Oda river, that were inserted into the model to perform a second simulation of the river basin. The area of the maximum simulated depth was then verified with the estimated flood area based on GSI maps for the Mabicho region. The results indicated that the simulated and estimated observations were consistent. This type of analysis may be a good reference to understand flooding situations caused by embankment failure and backwater effects due to extreme events.

We also verified the flood inundation extent profile, particularly over the Mabicho district, for different time periods. We observed a maximum flood extent profile between 14:00 JST on 6 July and 12:00 JST on 7 July 2018. The RRI model does not include inputs regarding embankment failure and backwater effects. We included those effects, based on a simple assumption that such an approach should be incorporated in any hydrological model to accurately understand flood scenarios of a river basin.

Japan has experienced numerous episodes of flooding due to embankment failure during extreme rain events, which has resulted in catastrophic damage and other consequences. The number of man-made river embankments has increased globally, especially in urbanized areas. The consideration of flood scenarios in the Oda river basin, improvements to data on river geometries, and adoption of new ideas based on reliable simulations of flood affects can be valuable references for the proper management of global water resources.

Author Contributions: Conceptualization, methodology, and formal analysis, S.P.C.; investigation, S.P.C., H.K., and R.M.; writing—original draft preparation, S.P.C.; writing—review and editing, S.P.C., H.K., and R.M.; supervision, R.M. All authors have read and agreed to the published version of the manuscript.

Funding: This research was funded by the internal project under the Storm, Flood and Landslide Research Division, National Research Institute for Earth Science and Disaster Resilience (NIED), Tsukuba, Japan.

Acknowledgments: Authors are thankful to the Ministry of Land, Infrastructure, Transport, and Tourism (MLIT), Japan Meteorological Agency (JMA), Geospatial Information Authority of Japan (GSI), and Conservation Science Program of World Wildlife Fund (WWF) for publishing and updating the important information and related data sets in their webpages. The authors acknowledge the support of the NIED. The authors would like to thank the anonymous reviewers for their constructive comments on our paper.

Conflicts of Interest: The authors declare no conflict of interest.

References

1. Hirabayashi, Y.; Kanae, S. First estimate of the future global population at risk of flooding. *Hydrol. Res. Lett.* **2009**, *3*, 6–9. [CrossRef]
2. Doocy, S.; Daniels, A.; Murray, S.; Kirsch, T.D. The human impact of floods: A historical review of events 1980-2009 and systematic literature review. *PLoS Curr.* **2013**, 5. [CrossRef] [PubMed]
3. Kundzewicz, Z.W.; Szwed, M.; Pińskwar, I. Climate variability and floods—A global review. *Water* **2019**, *11*, 1399. [CrossRef]
4. Okazaki, A.; Yeh, P.J.-F.; Yoshimura, K.; Watanabe, M.; Kimoto, M.; Oki, T. Changes in flood risk under global warming estimated using MIROC5 and the Discharge Probability Index. *J. Meteorol. Soc. Jpn.* **2012**, *990*, 509–524. [CrossRef]
5. Hirabayashi, Y.; Mahendran, R.; Koirala, S.; Konoshima, L.; Yamazaki, D.; Watanabe, S.; Kim, H.; Kanae, S. Global flood risk under climate change. *Nat. Clim. Chang.* **2013**, *3*, 816–821. [CrossRef]
6. Nakamura, M.; Kaneda, S.; Wakazuki, Y.; Muroi, C.; Hashimoto, A.; Kato, T.; Noda, A.; Yoshizaki, M.; Yasunaga, K. Effects of global warming on heavy rainfall during the Baiu season projected by a cloud-system-resolving model. *J. Disaster Res.* **2008**, *3*, 15–24. [CrossRef]
7. Mouri, G.; Minoshima, D.; Golosov, V.; Chalov, S.; Seto, S.; Yoshimura, K.; Nakamura, S.; Oki, T. Probability assessment of flood and sediment disasters in Japan using the total runoff-integrating pathways model. *Int. J. Disaster. Risk Reduct.* **2013**, *3*, 31–43. [CrossRef]
8. Tominaga, A. Lessons learned from Tokai heavy rainfall. *J. Disaster Res.* **2007**, *2*, 50–53. [CrossRef]

9. Sato, T.; Fukuzono, T.; Ikeda, S. The Niigata Flood in 2004 as a Flood Risk of Low Probability but High Consequence. In *A Better Integrated Management of Disaster Risks: Toward Resilient Society to Emerging Disaster Risks in Mega-Cities*; TERRAPUB and NIED: Tokyo, Japan, 2006; pp. 177–192.
10. PC, S.; Misumi, R.; Nakatani, T.; Iwanami, K.; Maki, M.; Maesaka, T.; Hirano, K. Accuracy of quantitative precipitation estimation using operational weather radars: A case study of heavy rainfall on 9-10 September 2015 in the East Kanto Region, Japan. *J. Disaster Res.* **2016**, *11*, 1003–1016. [CrossRef]
11. PC, S.; Nakatani, T.; Misumi, R. Hydrological simulation of small river basins in northern Kyushu, Japan, during the extreme rainfall event of July 5–6, 2017. *J. Disaster Res.* **2018**, *13*, 396–409. [CrossRef]
12. Cabinet Office. Japan. Report on Damages by the Heavy Rain Event of July (in Japanese). 2019. Available online: http://www.bousai.go.jp/updates/h30typhoon7/pdf/310109_1700_h30typhoon7_01.pdf. (accessed on 17 May 2019).
13. Mainichi, Japan. 'Backwater Phenomenon' Linked to Deadly Flood in Okayama Prefecture: Experts. Available online: https://mainichi.jp/english/articles/20180711/p2a/00m/0na/009000c. (accessed on 18 February 2019).
14. Sayama, T.; Ozawa, G.; Kawakami, T.; Nabesaka, S.; Fukami, K. Rainfall-runoff-inundation analysis of the 2010 Pakistan flood in the Kabul River basin. *Hydrol. Sci. J.* **2012**, *57*, 298–312. [CrossRef]
15. Sriariyawat, A.; Pakoksung, K.; Sayama, T.; Tanaka, S.; Koontanakulvong, S. Approach to estimate the flood damage in Sukhothai Province using flood simulation. *J. Disaster Res.* **2013**, *8*, 406–414. [CrossRef]
16. Nastiti, K.D.; Kim, Y.; Jung, K.; An, H. The application of rainfall-runoff-inundation (RRI) model for inundation case in upper Citarum watershed, West Java-Indonesia. *Procedia Eng.* **2015**, *125*, 166–172. [CrossRef]
17. Yoshimoto, S.; Amarnath, G. Applications of satellite-based rainfall estimates in flood inundation modeling—A case study in Mundeni Aru River Basin, Sri Lanka. *Remote Sens.* **2017**, *9*, 998. [CrossRef]
18. PC, S.; Nakatani, T.; Misumi, R. Analysis of flood inundation in ungauged mountainous river basins: A case study of an extreme rain event on 5–6 July 2017 in northern Kyushu, Japan. *J. Disaster Res.* **2018**, *13*, 860–872. [CrossRef]
19. Saksena, S.; Merwade, V. Incorporating the effect of DEM resolution and accuracy for improved flood inundation mapping. *J. Hydrol.* **2015**, *530*, 180–194. [CrossRef]
20. Lehner, B.; Verdin, K.; Jarvis, A. *HydroSHEDS Technical Documentation*; World Wildlife Fund: Washington, DC, USA, 2006. Available online: http://hydrosheds.cr.usgs.gov (accessed on 20 February 2019).
21. Bhagabati, S.S.; Kawasaki, A. Consideration of the rainfall-runoff-inundation (RRI) model for flood mapping in a deltaic area of Myanmar. *Hydrol. Res. Lett.* **2017**, *11*, 155–160. [CrossRef]
22. Gichamo, T.Z.; Popescu, I.; Jonoski, A.; Solomatine, D. River cross-section extraction from the ASTER global DEM for flood modeling. *Environ. Model. Softw.* **2012**, *31*, 37–46. [CrossRef]
23. Fleischmann, A.; Paiva, R.; Collischonn, W. Can regional to continental river hydrodynamic models be locally relevant? A cross-scale comparison. *J. Hydrol. X* **2019**, *3*, 100027. [CrossRef]
24. López, P.L.; Sutanudjaja, E.H.; Schellekens, J.; Sterk, G.; Bierkens, M.F.P. Calibration of a large-scale hydrological model using satellite-based soil moisture and evapotranspiration products. *Hydrol. Earth Syst. Sci.* **2017**, *21*, 3125–3144. [CrossRef]
25. Abou Rafee, S.A.; Uvo, C.B.; Martins, J.A.; Domingues, L.M.; Rudke, A.P.; Fujita, T.; Freitas, E.D. Large-scale hydrological modelling of the upper Paraná River Basin. *Water* **2019**, *11*, 882. [CrossRef]
26. PC, S.; Nakatani, T.; Misumi, R. The role of the spatial distribution of radar rainfall on hydrological modeling for an urbanized river basin in Japan. *Water* **2019**, *11*, 1703. [CrossRef]
27. Scharffenberg, W. *Hydrological Modeling System HEC-HMS*; User's Manual; Publication of US Army Corps of Engineers: Davis, CA, USA, 2016.
28. Beven, K.J.; Lamb, R.; Quinn, P.F.; Romanowicz, R.; Freer, J. Top model. In *Computer Models of Watershed Hydrology*; Singh, V.P., Ed.; Water Resources Publications: Littleton, CO, USA, 1995; pp. 627–668.
29. Liang, X.; Lettenmaier, D.P.; Wood, E.F.; Burges, S.J. A simple hydrologically based model of land surface water and energy fluxes for general circulation models. *J. Geophys. Res.* **1994**, *99*, 14415–14428. [CrossRef]
30. Manfreda, S.; Fiorentino, M.; aIacobellis, V. DREAM: A distributed model for runoff, evapotranspiration, and antecedent soil moisture simulation. *Adv. Geosci.* **2005**, *2*, 31–39. [CrossRef]
31. Bhattacharya, B.; Mazzoleni, M.; Ugay, R. Flood inundation mapping of the sparsely gauged large-scale Brahmaputra Basin using remote sensing products. *Remote Sens.* **2019**, *11*, 501. [CrossRef]

32. Yoon, S.-S. Adaptive blending method of radar-based and numerical weather prediction QPFs for urban flood forecasting. *Remote Sens.* **2019**, *11*, 642. [CrossRef]
33. Haque, M.M.; Seidou, O.; Mohammadian, A.; Djibo, A.G.; Liersch, S.; Fournet, S.; Karam, S.; Perera, E.D.P.; Kleynhans, M. Improving the accuracy of hydrodynamic simulations in data scarce environments using Bayesian model averaging: A case study of the inner Niger Delta, Mali, West Africa. *Water* **2019**, *11*, 1766. [CrossRef]
34. Li, J.; Li, T.; Liu, S.; Shi, H. An efficient method for mapping high-resolution global river discharge based on the algorithms of drainage network extraction. *Water* **2018**, *10*, 533. [CrossRef]
35. Lehner, B.; Verdin, K.; Jarvis, A. New global hydrography derived from spaceborne elevation data. *EOS Trans. Am. Geophys. Union* **2008**, *89*, 93–94. [CrossRef]
36. Grimaldi, S.; Li, Y.; Walker, J.P.; Pauwels, V.R.N. Effective representation of river geometry in hydraulic flood forecast models. *Water Resour. Res.* **2018**, *54*, 1031–1057. [CrossRef]
37. PC, S.; Kamimera, H. Flooding in Oda River Basin during torrential rainfall event in July 2018. *Eng. J.* **2019**, *23*, 477–485. [CrossRef]
38. Tam, T.H.; Abd Rahman, M.Z.; Harun, S.; Hanapi, M.N.; Kaoje, I.U. Application of Satellite rainfall products for flood inundation modelling in Kelantan River Basin, Malaysia. *Hydrology* **2019**, *6*, 95. [CrossRef]
39. Miyano, M.; Komoto, Y.; Utsumi, T. Survey on Disaster Due to the Heavy Rain in July 2018–Mabi-cho, Kurasshiki City. Institute of Social Safety Science. *Annu. Summ.* **2018**, *43*, 61–62. (In Japanese)
40. Yuan, F.; Zhang, L.; Soe, K.M.W.; Ren, L.; Zhao, C.; Zhu, Y.; Jiang, S.; Liu, Y. Applications of TRMM- and GPM-Era multiple-satellite precipitation products for flood simulations at sub-daily scales in a sparsely gauged watershed in Myanmar. *Remote Sens.* **2019**, *11*, 140. [CrossRef]
41. Maki, M.; Iwanami, K.; Misumi, R.; Park, S.-G.; Moriwaki, H.; Maruyama, K.; Watabe, I.; Lee, D.-I.; Jang, M.; Kim, H.-K.; et al. Semi-operational rainfall observations with X-band multi-parameter radar. *Atmos. Sci. Lett.* **2005**, *6*, 12–18. [CrossRef]
42. Sharma, S.K.; Kwak, Y.-J.; Kumar, R.; Sarma, B. Analysis of hydrological sensitivity for flood risk assessment. *ISPRS Int. J. Geo-Inf.* **2018**, *7*, 51. [CrossRef]
43. Sayama, T. *Rainfall-Runoff-Inundation (RRI) Model*; Disaster Prevention Research Institute (DPRI), Kyoto University: Kyoto, Japan, 2017.
44. Leopold, L.B.; Maddock, T.J. The hydraulic geometry of stream channels and some physiographic implications. *U.S. Geol. Surv. Prof. Pap.* **1953**, *252*, 1–57. [CrossRef]
45. Gupta, H.V.; Kling, H.; Yilmaz, K.K.; Martinez, G.F. Decomposition of the mean squared error and NSE performance criteria: Implications for improving hydrological modelling. *J. Hydrol.* **2009**, *377*, 80–91. [CrossRef]
46. MLIT. The Second Takahashi River Water System Oda River Levee Investigation Committee. 2018. Available online: http://www.cgr.mlit.go.jp/emergency/2018/pdf/02odagawahaifu.pdf (accessed on 22 April 2019). (In Japanese)
47. Maesaka, T.; Maki, M.; Iwanami, K. Operational Rainfall Estimation by X-band MP Radar Network in MLIT, Japan. In Proceedings of the 35th Conference on Radar Meteorology, Pittsburgh, PA, USA, 26–30 September 2011.
48. Yamazaki, D.; Ikeshima, D.; Sosa, J.; Bates, P.D.; Allen, G.H.; Pavelsky, T. MERIT Hydro: A high-resolution global hydrography map based on latest topography datasets. *Water Resour. Res.* **2019**, *55*, 5053–5073. [CrossRef]
49. Tadono, T.; Nagai, H.; Ishida, H.; Oda, F.; Naito, S.; Minakawa, K.; Iwamoto, H. Generation of the 30 M-MESH global digital surface model by ALOS PRISM. *Int. Arch. Photogramm. Remote Sens. Spat. Inf. Sci.* **2016**, *XLI-B4*, 157–162. [CrossRef]
50. Bates, P.D.; Marks, K.J.; Horritt, M.S. Optimal use of high-resolution topographic data in flood inundation models. *Hydrol. Process.* **2003**, *17*, 537–557. [CrossRef]